Aging assessment of large generator insulation based on PD measurements*

YUE Bo[1,2,3**], CHEN Xiaolin[1], CHENG Yonghong[1] and XIE Hengkun[1***]

(1. State Key Laboratory of Electrical Insulation and Power Equipment, Xi'an Jiaotong University, Xi'an 710049, China; 2. Graduate School at Shenzhen, Tsinghua University, Shenzhen 518055, China; 3. Department of Electrical Engineering, Tsinghua University, Beijing 100084, China)

Received December 14, 2004; revised May 27, 2005

Abstract The statistical parameters of phase resolved partial discharge (PD) distribution and ultra-wideband (UWB) characteristics of PD pulse are proposed for aging assessment of large generator insulation. Multi-stress aging tests of the model generator stator bar specimens were performed and PD measurements were conducted using both digital PD detector with frequency ranging from 40 kHz to 400 kHz and UWB PD detector with bandwidth from 10 MHz to 3 GHz at different aging stages. The test results show that the skewness and UWB frequency characteristics of PD can be taken as the characterization parameters for aging assessment of generator insulation. Furthermore, the measurement results of real generator stator bars show that these methods based on statistical parameters and UWB characteristics of PD are prospective for aging assessment and residual lifetime estimation of large generator stator insulation.

Keywords: partial discharge, stator insulation, multi-stress accelerated aging, statistical parameters, ultra-wideband, aging assessment.

Aging assessment of generator insulation is of great significance in planning the effective outage and maintenance. In the last decade, aging assessment of large generator insulation was a research area of great interest[1—5]. A number of papers have been published on the techniques of insulation condition diagnosis and aging assessment of generator insulation. Nearly all these studies rely on electrical measurements and most of them pay much attention to analysis of the characteristics of the partial discharge signal derived from generator. The most widely used parameter of partial discharge is the maximum partial discharge (PD) magnitude (q_{max}). However, whether this parameter is specific to some insulation system and testing condition or not is still controversial[6—8]. Therefore, it is important to develop a test method capable of indicating the deterioration extent in insulation and finding the meaningful characterization parameters to evaluate the insulation condition. For this purpose, in this paper, aging tests of model bars under combined electrical, vibrational and thermal stresses are performed and several new characteristics are measured at different aging stages. Experimental results indicate that the aging of generator insulation may be characterized more exactly by the statistical parameter and the ultra-wideband (UWB) characteristics of PD, which is verified by the testing results of real generator stator bar insulation.

1 Experiment

1.1 Model stator bar specimens and accelerated aging tests

The model bars used in this work were replaced by stator coils of a 780 kW/6 kV electric motor that had served for 5 years. The insulation of the model bars was made of mica-epoxy with thickness of 3 mm, and the conductor of model bars was made of copper with cross section of 14.2 mm × 26.2 mm and length of 700 mm. For application of electrical stress, the insulation surface of the ends of the model bar specimens was coated with silicone carbide paint to suppress corona. The schematic diagram of the model stator specimen is shown in Fig. 1.

The multi-stress acceleration aging tests were conducted on the 42 model stator bars mentioned above by using a new aging testing set-up[9], which was able to provide a 50 Hz voltage up to 100 kV, heating temperature up to 300 ℃, vibration ampli-

* Supported by National Natural Science Foundation of China (Grant No. 59837260), China Postdoctoral Science Foundation (Grant No. 2004035041), and Opening Foundation of State Key Laboratory of Electrical Insulation and Power Equipment, Xi'an Jiaotong University, China

** To whom correspondence should be addressed. E-mail: yueb@sz.tsinghua.edu.cn

*** The author has passed away.

?1994-2018 China Academic Journal Electronic Publishing House. All rights reserved. http://www.cnki.net

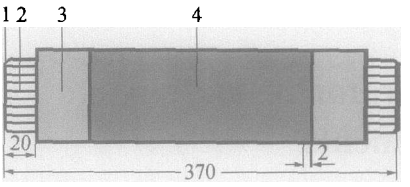

Fig. 1. Schematic diagram of the model stator specimen (unit: mm). 1, HV electrode; 2, copper strands; 3, SiC paint; 4, low resistance paint.

tude of 0—5 mm, vibration frequency of 0—10 kHz, thermal cycling temperature ranging from ambient temperature to 250 ℃, heating or cooling rate of 3—5 ℃/min.

The duration of the multi-stress aging test consists of a number of periods. One period includes a combination of thermal, electrical and mechanical stresses, which was performed at temperature of 155 ℃, electrical stress of 5.5 kV/mm, vibration frequency of 100 Hz, and amplitude of 1 mm for 96 hours and several thermal-cooling cycles, which were carried out with temperature increasing from ambient temperature to 155 ℃ in 30 minutes by heating and then decreasing to the ambient temperature in about 30 minutes by forced air convection for 24 hours. During the thermal-cooling cycling test, the bar specimens were relieved from the electrical and mechanical stresses temporarily. The multi-stress aging tests of stator bar specimens in this study spent more than 14 aging periods.

1.2 PD measurement system

1.2.1 Digital PD measurement system

The PD measurement system is shown in Fig. 2. The PD signal from the testing bar specimen is picked up by the measuring impedance and then fed through an analog amplifier (AKV572) to partial discharge analyzer (TE571). The measuring instruments are placed in a shielding room connected to the measuring impedance through high frequency coaxial cable with the characteristic impedance of 50 Ω.

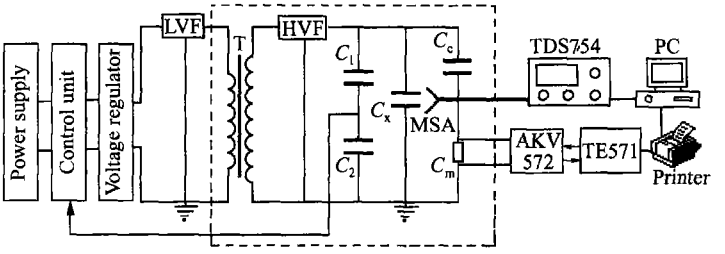

Fig. 2. Schematic diagram of the PD measurement system. LVF, low voltage filter; T, transformer; HVF, high voltage filter; C_x, specimen; C_c, coupling capacitor; C_m, measurement impedance; MSA, micro-strip antenna; TDS754, high speed digital oscilloscope; PC, personal computer; AKV572, analog amplifier; TE571, PD analyzer.

The TE571 PD analyzer, made by the HAEFELY TRENCH Company, is equipped with advanced hardware and powerful software. Its bandwidth has a lower limit of 40 kHz and an upper limit of 400 kHz. According to IEC 270, the PD pulses are integrated, and the maximum value of the integrated signal is proportional to the apparent charge. The PD measuring system is calibrated for each specimen before measurement with a standard calibrator.

1.2.2 UWB PD measurement system

The UWB PD detection system is also shown in Fig. 2. This UWB PD detector may measure the PD spectrum from 10 MHz to 3 GHz. The UWB PD detection circuit is the same as that for digital PD detection. However, the signals of PD pulses from the testing bar specimen are coupled to UWB PD detector by a micro-strip antenna. The standing wave ratio of the antenna is measured by using the HP8720C network analyzer with the sweep bandwidth of 20 GHz and the result of testing is shown in Fig. 3.

It can be found from Fig. 3 that the standing wave ratio of the antenna is 1.86 at 3 GHz and 2.6 at 4 GHz. It is well known that the influence of standing wave can be ignored when the ratio is less than 2, so the working bandwidth of the antenna is 3 GHz. The PD signals are sampled by a digital oscilloscope (Tektronix TDS 754) with a fast AD converter (ADC), and then transferred into the computer connected by GPIB bus. In order to ensure the matching of the system and avoid the oscillation of the pulse, the 50 Ω matching impedance is selected in the UWB testing system. With the UWB PD detection system, the waveforms of the PD signals from the testing specimen in both time domain and frequency domain can be obtained.

?1994-2018 China Academic Journal Electronic Publishing House. All rights reserved. http://www.cnki.net

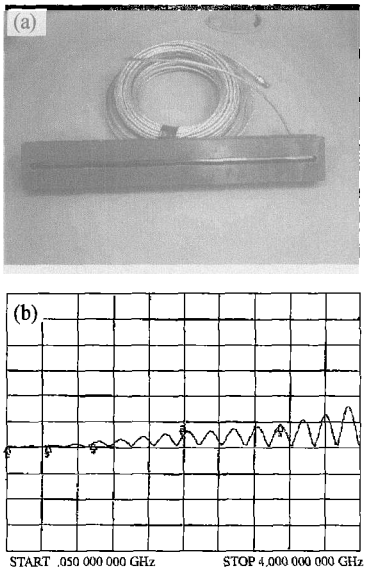

Fig. 3. UWB micro-strip antenna and its standing wave ratio. (a) UWB micro-strip antenna; (b) standing wave ratio of the antenna.

2 Test results

Over the multi-stress aging span, PD measurements were performed on the testing stator bar specimens after each aging period and a large set of data has been collected.

2.1 Phase resolved distribution of PD

By measuring the PD pulse distributions as a function of phase angle, it is possible to obtain information on the phenomena resulting in this distribution[10,11]. Previous studies have shown that the phase position of a discharge on the power frequency cycle can indicate the extent and mechanism of insulation deterioration[12]. A typical phase angle spectrum taken from one of the specimens is shown in Fig. 4.

It can be seen from Fig. 4 that the shapes of the maximum pulse height phase resolved distribution $H_{qmax}(\varphi)$, the mean pulse height phase resolved distribution $H_{qn}(\varphi)$, and the pulse count phase resolved distribution $H_n(\varphi)$ change with the aging time. However, it is difficult to quantitatively describe the changes in deterioration of the specimen insulation according to the phase resolved distributions of PD. Therefore, it is necessary to introduce the statistical parameters for analyzing the aging of insulation.

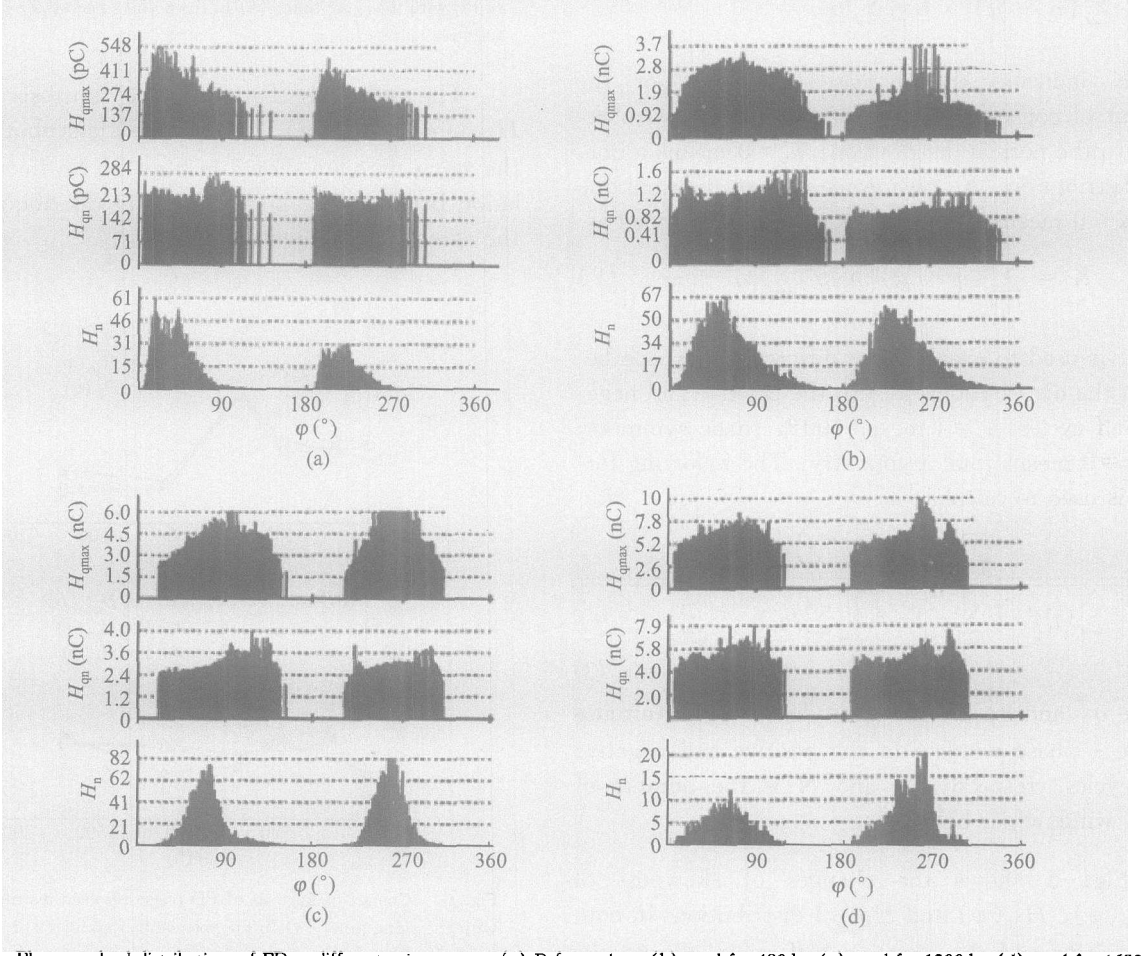

Fig. 4. Phase resolved distributions of PD at different aging stages. (a) Before aging; (b) aged for 480 h; (c) aged for 1200 h; (d) aged for 1680 h.

?1994-2018 China Academic Journal Electronic Publishing House. All rights reserved. http://www.cnki.net

2.2 Statistical parameter analysis

There are several statistical parameters used to evaluate the insulation condition based on the shapes of $H_{qmax}(\varphi)$, $H_{qn}(\varphi)$ and $H_n(\varphi)$[10,11,13], such as the skewness S, kurtosis K, cross-correlation factor c, discharge factor Q, the number of peaks n_p and so on. It has been found that S, K and c had a certain relation with the insulation condition in our aging tests.

S describes the asymmetry of a distribution with respect to a normal distribution. $S=0$ means symmetric, $S>0$ means asymmetric with the left side large, and $S<0$ means asymmetric with right side large. S is defined as

$$S = \sum_{i=1}^{N}(q_i-\mu)^3 p_i \Big/ \sigma^3 \sum_{i=1}^{N} p_i, \qquad (1)$$

where q_i is the recorded PD value and p_i is the probability of frequency of appearance for that value q_i in the time window i, μ is the mean value $\mu = \sum q_i \cdot p_i \Big/ \sum p_i$, and σ is calculated by $\sigma^2 = \sum (q_i-\mu)^2 \cdot p_i \Big/ \sum p_i$.

K indicates the increased sharpness or the amount of concentration of the distribution with respect to the normal distribution. $K=0$ means a normal distribution, $K>0$ means a sharp distribution, and $K<0$ means a flat distribution. K is defined as

$$K = \sum_{i=1}^{N}(q_i-\mu)^4 p_i \Big/ \sigma^4 \sum_{i=1}^{N} p_i - 3. \qquad (2)$$

c is used to evaluate the difference in shape between the distributions both in the positive and negative half cycles. $c=1$ means 100% shape symmetry and $c=0$ means total asymmetry. The following formula is used to calculate c

$$c = \frac{\sum_{i=1}^{N} q_i^+ q_i^- - \sum_{i=1}^{N} q_i^+ \sum_{i=1}^{N} q_i^- \Big/ N}{\sqrt{\left[\sum_{i=1}^{N}(q_i^+)^2 - \left(\sum_{i=1}^{N} q_i^+\right)^2 \Big/ N\right]\left[\sum_{i=1}^{N}(q_i^-)^2 - \left(\sum_{i=1}^{N} q_i^-\right)^2 \Big/ N\right]}}, \qquad (3)$$

where q_i^+ and q_i^- are the mean discharge magnitudes in the i phase window in the positive and negative half cycles, respectively, and N is the number of phase window per half cycle.

Fig. 5 shows the changes of skewness of $H_{qmax}(\varphi)$, $H_{qn}(\varphi)$ and $H_n(\varphi)$ distributions in both the positive and the negative half cycles during the aging test. Each point in Fig. 5 represents the skewness obtained at the applied voltages of 6 kV. It is quite obvious that the skewness decreases with the aging time in the positive half cycle or in the negative half cycle, and the skewness decreases to the negative value of -0.1—-0.2 after 1680 h of aging.

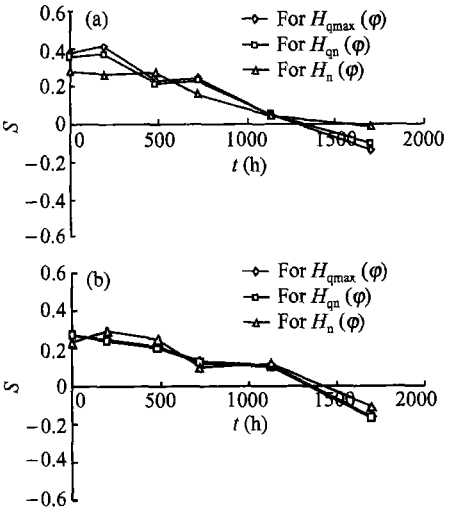

Fig. 5. Change of skewness of the phase resolved distributions S of PD with the aging time. (a) In the positive half cycle; (b) in the negative half cycle.

The relations between the kurtosis of the $H_{qmax}(\varphi)$, $H_{qn}(\varphi)$, and $H_n(\varphi)$ distributions and the aging time are shown in Fig. 6. No linear correlation between the kurtosis of PD distributions and the aging time is found.

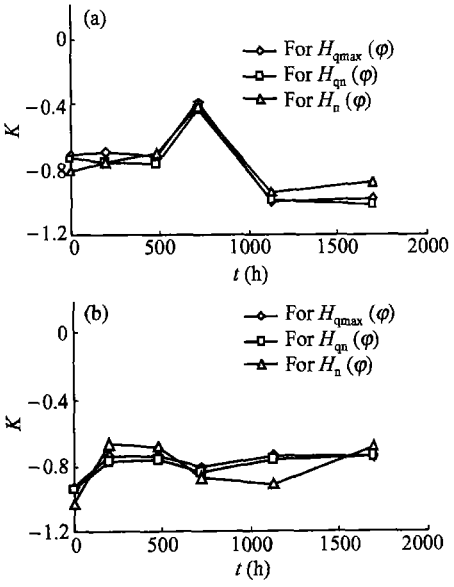

Fig. 6. Change of kurtosis of PD phase resolved distributions K with the aging time. (a) In the positive half cycle; (b) in the negative half cycle.

?1994-2018 China Academic Journal Electronic Publishing House. All rights reserved. http://www.cnki.net

Fig. 7 shows the change of the cross-correlation factor of the PD phase resolved distributions with the aging time. It can be seen that the cross-correlation factor of the $H_{qmax}(\varphi)$, $H_{qn}(\varphi)$ and $H_n(\varphi)$ distributions decreases non-monotonously with the aging time. In other words, the asymmetric degree of $H_{qmax}(\varphi)$, $H_{qn}(\varphi)$ and $H_n(\varphi)$ distributions increases with the aging time.

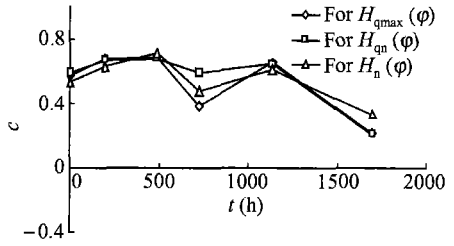

Fig. 7. Change of c of the phase resolved distributions of PD with the aging time.

2.2 Discharge magnitude analysis

The changes of the discharge magnitude with the aging time of 5 stator bar specimens are represented in Fig. 8. It can be seen that the maximum magnitudes of PD in the positive half cycle are very similar to that in the negative half cycle. The maximum magnitude of PD of the stator bar specimens increases with the aging time.

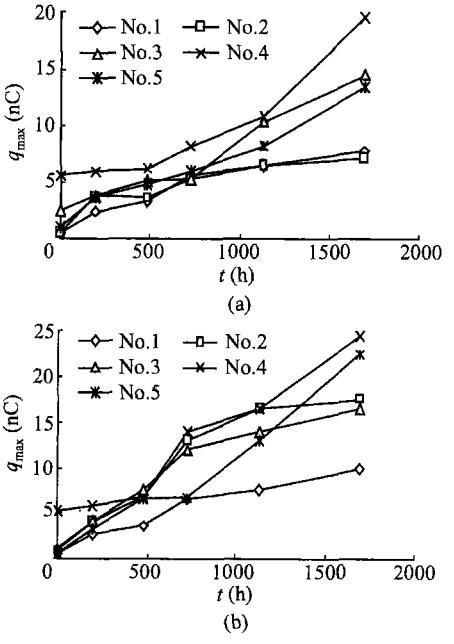

Fig. 8. Change of maximum magnitude q_{max} of PD with the aging time. (a) In the positive half cycle and (b)in the negative half cycle.

2.3 Change of the UWB characteristics of the PD pulse

A typical example of the UWB PD pulse in the time domain of the stator bar specimens at different aging stages is shown in Fig. 9.

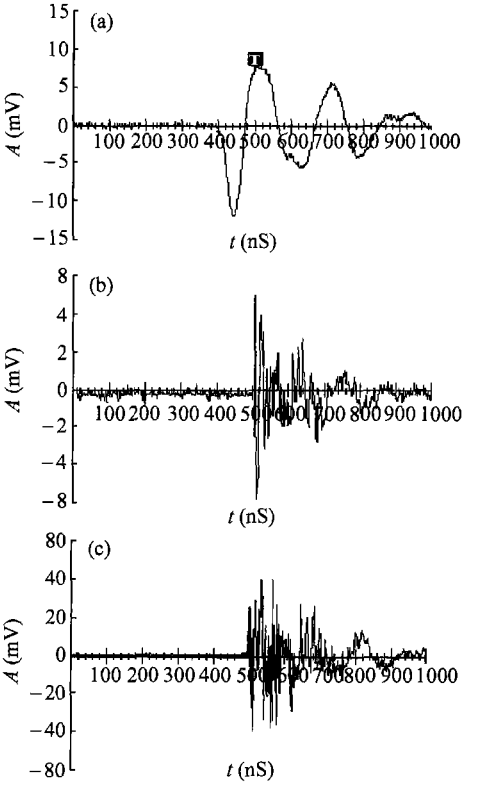

Fig. 9. The UWB characteristics of the PD pulse in the time domain of the stator bar specimen at different aging stages (A is the voltage amplitude of the PD pulse). (a) Before aging; (b) after 1200 h of multi-stress aging; (c) after 1680 h of multi-stress aging.

From Fig. 9, it can be seen that the rise time of the UWB PD pulse is between 200 ps and 35 ns with the pulse duration of about 400 ns, and both the rise time and duration of the UWB PD pulse decrease with the aging time. The PD pulse at the early aging stage is stable, whereas the pulse after long aging time, especially at the final aging stage, contains abundant high frequency components.

Although some changes of the UWB pulse in the time domain appear at different aging stages, it is difficult to analyze quantitatively the information on aging. Therefore, it is necessary to analyze the characteristics of the UWB PD pulse in the frequency domain.

As is well known, the frequency representation

?1994-2018 China Academic Journal Electronic Publishing House. All rights reserved. http://www.cnki.net

of the no-period signal $x(t)$ is

$$x(t) = \frac{1}{2\pi}\int_{-\infty}^{\infty} X(\omega)\exp(j\omega t)d\omega, \quad (4)$$

where

$$X(\omega) = \int_{-\infty}^{\infty} x(t)\exp(j\omega t)dt. \quad (5)$$

Equation (5) is named the continuous time Fourier transform. $X(\omega)$ is the measure of the similarity between the signal $x(t)$ and the complex sinusoidal functions.

The UWB PD signals were detected by digital oscilloscope and transformed simultaneously to the frequency spectrum in the frequency domain based on Eq. (5). The frequency waveforms corresponding to the UWB PD pulses in the time domain are shown in Fig. 10.

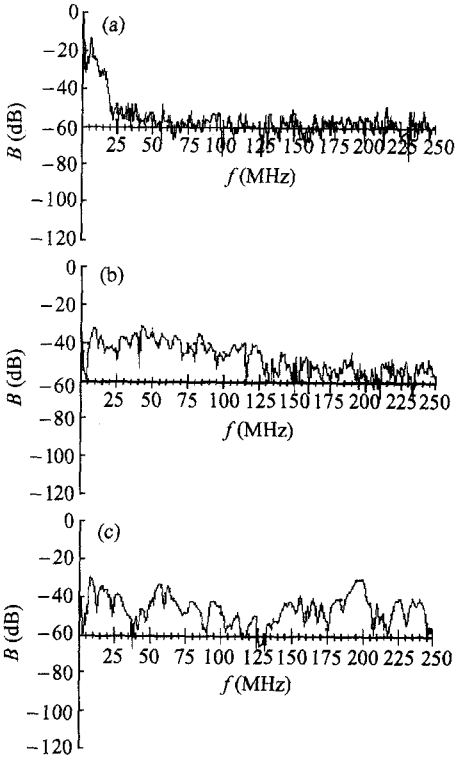

Fig. 10. Frequency spectrum of UWB PD pulse at different aging stages (B is the amplitude of the frequency spectrum of the PD pulse). (a) Before aging; (b) after 1200 h of multi-stress aging; (c) after 1680 h of multi-stress aging.

From Fig. 10, it can be seen that the high frequency components contained in the UWB PD pulse concentrate on the frequency bands from 5 to 25 MHz at the early aging stage, and the high frequency components increase with the aging time. And at the final aging stage, the high frequency components are distributed over the frequency range of 5 MHz to 250 MHz. However, it should be pointed out that the UWB frequency response will be strongly modified and the pulse shape may change due to the pulse propagation in a real winding. So the pulse shape and frequency response of the real stator winding may be different from those of model stator bar specimen to some extent.

2.4 Relations between S, q_{max} and the breakdown voltage (U_{BD})

After PD measurements, breakdown tests of 6 stator bars specimens were carried out at the end of each aging period. The relations between the skewness and breakdown voltage and between the maximum magnitude of PD and breakdown voltage are shown in Figs. 11 and 12, respectively.

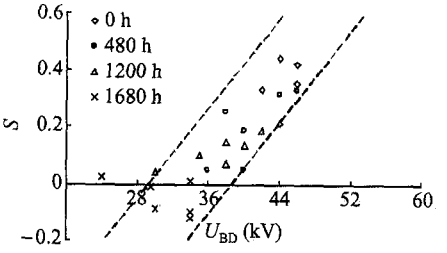

Fig. 11. Relation between S and U_{BD}.

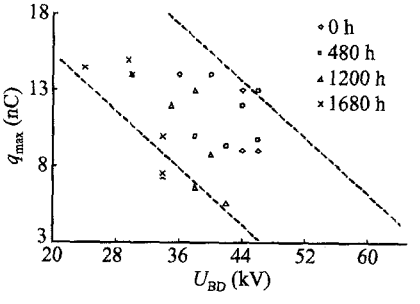

Fig. 12. Relation between q_{max} and U_{BD}.

3 Discussion

The experimental results of digital PD measurements indicate that the statistical analysis of the acquired PD distributions is meaningful for aging assessment of the stator bar insulation. Compared with K and c, the skewnesses of the $H_{qmax}(\varphi)$, $H_{qn}(\varphi)$ and $H_n(\varphi)$ distributions both in the positive and negative half cycles are more sensitive to the change of PD activities occurring in the insulation of the stator bar specimens during the aging testing process. Fig. 5 shows that the phase distribution of PD is skewed to the left (with positive value of skewness) at the early

?1994-2018 China Academic Journal Electronic Publishing House. All rights reserved. http://www.cnki.net

aging stage. As aging develops to a certain extent, the skewness approaches zero. Further aging makes the distribution skewed to the right (with the negative value of skewness). Therefore, the skewness may be taken as a characterization parameter of the aging of the stator insulation. Figs. 6 and 7, however, indicate that other statistical parameters such as the kurtosis and cross-correlation factor do not exhibit linear relation to the aging of the stator insulation. Fig. 8 demonstrates that the maximum magnitude of PD (q_{max}) increases with aging. However, the q_{max} value of each stator bar specimen scatters largely, especially at the later stage of aging. Because of the scatteration of q_{max} in our experiment, it seems that q_{max} is inappropriate to evaluate the aging status of the model stator bar employed in this paper. However, more experiments and data are needed to verify whether this conclusion is suitable for other types of stator bar.

In order to develop a method for estimating the residual lifetime of stator insulation, breakdown tests were also performed on the stator bar specimens. It is found that the skewness decreases continuously with the aging time (aging extent), and the electrical strength decreases to 7—10 kV/mm when the skewness decreases to the negative value of -0.1—-0.2. Usually, the insulation of the large generator stator bar is required to have electrical strength higher than 6 kV/mm—7 kV/mm in the preventive maintenance test. Therefore, skewness of -0.1—-0.2 may be adopted as a criterion of serious aged stator insulation.

According to Eq. (1), the decrease of the skewness indicates that the phase resolved distributions of PD skews to the right, that is to say, a large proportion of PD takes place at the larger phase position corresponding to higher instantaneous voltage. In addition, this kind of phase distribution of PD implies the increase of the cavity number and size along the electric field, which can result in the decrease of the effective thickness of the stator bar and the increase of the breakdown probability when discharge takes place in cavity. Therefore, the theoretical analysis demonstrates that the decrease of skewness indicates the aging of the stator bar, which is in agreement with the experimental results.

The PD pulse of the generator stator insulation is a fundamental event with a duration of as short as a few ns, which has a very wide frequency spectrum up to GHz. Compared with the conventional PD detection with narrow bandwidth from 10 kHz to 1 MHz, PD detection with UWB method may provide more information on the aging of stator bar insulation. Fig. 9 indicates that the UWB PD pulse has the rise time between 200 ps and 35 ns, and the pulse duration of about 400 ns, which are different from the conclusion of Stone et al.[14]. It probably results from differences in the measurement environments and testing specimens. From Fig. 9, it can be seen that the rise time and duration of the UWB PD pulse decrease with the aging time. Although the PD pulse at the early aging stage is stable, PD pulse contains more and more high frequency component as the aging becomes more and more serious.

Although some changes of the UWB PD pulse in the time domain appear in Fig. 9 at different aging stages, it is difficult to quantitatively analyze the aging. On the contrary, the changes of the UWB PD pulse in the frequency domain may reflect the aging of stator insulation. As is shown in Fig. 10, the high frequency component contains UWB PD pulse concentrated on the frequency ranging from 5 to 25 MHz at the early aging stage. The frequency components increase with the aging time, and the frequency components are distributed over the frequency ranging from 5 to 250 MHz at the final aging stage. Therefore, the UWB frequency characteristics of PD may be used for aging assessment of stator insulation.

The relation between the aging and the frequency spectrum of PD has been intensively studied. Both the increase of the size along the electric field and the connection of small defects with aging will result in increase of the inception discharge voltage. And at the same time, the ablation of the discharge tip and the formation of semi-conductive layer at the cavity wall will also result in the increase of the discharge voltage, which will correspondingly reduce the wave front of the PD pulse. Moreover, the inactive gas produced during the discharge process will result in the increase of pressure and the dielectric strength of the cavity which can shorten the width of the discharge wave front. Consequently, these factors mentioned above will lead to the occurrence of high frequency components in the PD frequency spectrum. Our experiment results are consistent with the above theoretical analysis.

In order to clarify the availability of the skewness of PD distribution and UWB frequency charac-

?1994-2018 China Academic Journal Electronic Publishing House. All rights reserved. http://www.cnki.net

teristics for aging assessment of real generator stator insulation, PD testes were performed on several stator bars taken from four real generators of 300 MW/18 kV, which had severed for 0, 16, 18 and 23 years, respectively. The real stator bars are shown in Fig. 13. The test results are shown in Figs. 14 and 15.

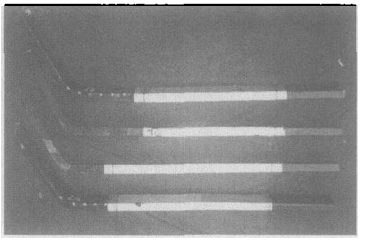

Fig. 13. Real generator stator bar specimens.

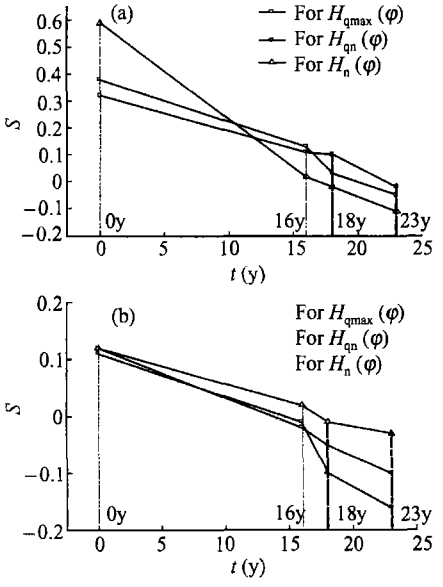

Fig. 14. Skewnesses of PD phase resolved distributions S of the real stator bars of generators serving for 0, 16, 18 and 23 years, respectively. (a) In the positive half cycle; (b) in the negative half cycle.

From Figs. 14 and 15, it can be seen that the longer the service time of the stator bar is, the smaller the skewness and the higher the frequency of the high frequency components contained in the UWB frequency spectrum are. The variation trend of the skewness and UWB characteristics with service time is consistent with the experimental results of model stator bar specimens. The skewness of stator bar serving for 23 years lowers down to -0.1 and its high frequency components appear at about 250 MHz. According to the criterion of aging assessment mentioned above, the insulation of this stator bar is aged seriously. The criterion of aging assessment is proved highly effective by the breakdown testing results. The breakdown voltage of this bar lowers down to 30 kV, which is much lower than the test voltage of preventive maintenance test (45 kV). Therefore, the results verify that the skewness of the phase resolved distributions of PD and the UWB frequency characteristics of the PD pulse signal are useful for aging assessment of generator stator insulation.

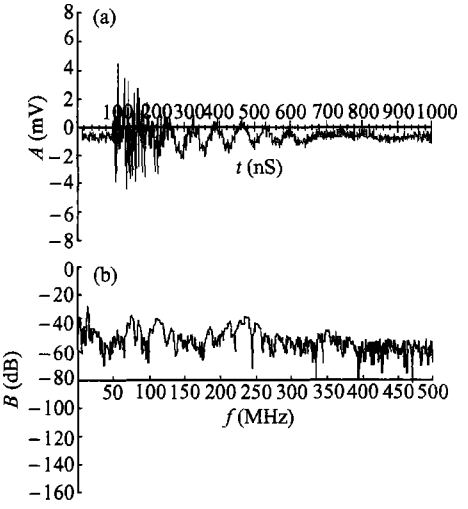

Fig. 15. The UWB characteristics of PD pulse of the real stator bar of generator serving for 23 years. (a) In the time domain; (b) in the frequency domain.

4 Conclusion

Based on the statistical parameters of the PD phase resolved distributions and the UWB frequency characteristics of the model stator bars and real stator bars, the following conclusions can be drawn.

(i) The skewnesses (S) of the $H_{qmax}(\varphi)$, $H_{qn}(\varphi)$ and $H_n(\varphi)$ distributions decreases from positive to negative value and the maximum PD magnitude (q_{max}) increases with the aging time.

(ii) When the skewness lowers down to -0.1—-0.2, the stator bar insulation is seriously aged.

(iii) It is difficult to assess the aging of the model stator bar specimen based on the q_{max} value alone due to the large scatters of different specimens in our experiment. However, more experiment and data are needed to verify whether the conclusion is suitable for other types of stator bar.

(iv) The relations among K and c of the $H_{qmax}(\varphi)$, $H_{qn}(\varphi)$ and $H_n(\varphi)$ distributions and the

?1994-2018 China Academic Journal Electronic Publishing House. All rights reserved. http://www.cnki.net

aging time are not suitable for aging assessment of large generator stator insulation according to our experiment results.

(v) The change of the UWB PD pulse in the frequency domain may reflect the aging status. The high frequency components contained in UWB PD pulse increase with the aging time. The appearance of the higher frequency component (for example, 250 MHz) indicates that the stator insulation is aged seriously. However, it should be pointed out that the conclusion about UWB frequency spectrum and pulse shape would be strongly modified by pulse propagation and distortion in a real stator winding.

References

1 Kimura K. Progress of insulation aging and diagnostics of high voltage rotating machine windings in Japan. IEEE Electrical Insulation Magazine, 1993, 9(3): 13—20.

2 Kimura K. and Kaneda Y The role of microscopic defects in multistress aging of micaceous insulation. IEEE Transactions on Dielectrics and Electrical Insulation, 1995, 2(3): 426—432.

3 Stone G.C , Gupta B.K., Lyles J.F. et al. Experience with accelerated aging tests on stator bars and coils. In: Conference Record of 1990 IEEE International Symposium on Electrical Insulation. Toronto, Canada, June 3—6, 1990, 356—360.

4 Yue B., Zhang X.H. and Lu W.S. Study on multi-factor aging characteristics of motor stator windings. High Voltage Engineering (in Chinese), 2000, 26(2): 3—7.

5 Yue B., Li J. and Zhang L. Study on developing law of AC current parameters of epoxy-mica insulation during the process of multifactors aging of stator bars. Power System Technology (in Chinese), 2001, 25(3): 30—33

6 Kheirmand A., Leijon M. and Gubanski S.M. New practices for partial discharge detection and localization in large rotating machines. IEEE Transactions on Dielectrics and Electrical Insulation, 2003, 10(6): 1042—1052.

7 Anders G.J., Endrenyi J., Ford G.L. et al. A probabilistic model for evaluating the remaining life of evaluating the remaining life of electrical insulation in rotating machines. IEEE Transactions on Energy Conversion, 1990, 5(4): 761—767.

8 Stone G.C., Sedding H.G., Lloyd B.A. et al. The ability of diagnostic tests to estimate the remaining life of stator insulation. IEEE Transactions on Energy Conversion, 1988, 3(4): 833—841.

9 Yue B., Song J.C. and Xie H.K. Study on multi-stress aging test system for stator winding insulation of large generator. Proceedings of the CSEE (in Chinese), 2000, 20(7): 9—13.

10 Gulski E. and Kreuger F H. Computer-aided recognition of discharge sources. IEEE Transactions on Dielectrics and Electrical Insulation, 1992, 27(1): 82—92.

11 Gulski E. Computer-aided measurement of partial discharges in HV equipment. IEEE Transactions on Dielectrics and Electrical Insulation, 1993, 28(6): 969—983.

12 Guastavino F. and Cerutti B. Tree growth monitoring by means of digital partial discharge measurements. IEEE Transactions on Dielectrics and Electrical Insulation, 2003, 10(1): 65—72.

13 Yue B., Li J. and Zhang X.H. Study on multi-stress aging of epoxy-mica insulation based on fingerprint parameters. Advanced Technology of Electrical Engineering and Energy (in Chinese), 2001, 20(2): 29—32.

14 Stone G.C., Sedding H.G., Fujimoto N. et al. Practical implementation of ultra wide band partial discharge detectors IEEE Transactions on Dielectrics and Electrical Insulation, 1992, 27(1): 70—81.

?1994-2018 China Academic Journal Electronic Publishing House. All rights reserved. http://www.cnki.net